Experimental study of freely falling thin disks: Transition from planar zigzag to spiral

Hongjie Zhong, Shiyi Chen, and Cunbiao Lee

View Online

Export Citation

Experimental study of freely falling thin disks: Transition from planar zigzag to spiral

Hongjie Zhong, Shiyi Chen, and Cunbiao Lee[a)]
State Key Laboratory for Turbulence and Complex Systems, College of Engineering, Peking University, Beijing 100871, China

Using a stereoscopic vision method, we have experimentally investigated the time evolution of a free thin disk motion with six degrees of freedom for the first time. It is found that, as the dimensionless moment of inertia I^* decreases, the trajectory of the disk transits from planar to nonplanar. New types of free falling motions were identified for small I^* values, including the spiral state and the transitional state. An extended $Re-I^*$ phase diagram corresponding to different flow regimes was given. The underlying physics associated with the transition is found to be connected to the interactions between the moving object and induced vortices. © 2011 American Institute of Physics. [doi:10.1063/1.3541844]

Free body motions in fluids are ubiquitous in nature. Such phenomena, including rising bubbles, falling leaves, paper sheets, and dispersal of winged seeds, exhibit complicated dynamical behaviors. The related studies can be dated back to the work of Newton and Maxwell. Over the past half century, this classic topic has received renewed interests in a wide range of contexts including meteorology,[1,2] sedimentology,[3,4] biomechanics,[5] chemical engineering,[6] and unsteady flapping aerodynamics.[7]

Due to interactions with the fluid flow, a free body does not generally select a rectilinear path. A variety of trajectories has been observed even for bodies with simple geometries, such as spheres and thin disks. Periodic oscillatory motion is the most common type and has been observed in flexible bodies such as bubbles, droplets, or solid bodies such as spheres, disks, or cones. For a free rising bubble in water, it is well known that its trajectory transits from zigzag to circular helix when the size exceeds a critical value.[8] However, for certain solid bodies, periodic oscillations are often observed to associate with planar motions. Field *et al.*[9] presented a phase diagram for thin disks based on the Reynolds number Re and dimensionless moment of inertia I^*. Steady falling, periodic oscillation, tumbling, and apparently chaotic motion were included in the phase diagram. These motions are similar to those found in the falling of two dimensional plates.[10–14]

An earlier study by Willmarth *et al.*[15] observed that the fluttering of a free falling disk may not reside in a vertical plane. Recent experiments on freely rising cylinders[16] also reported helical trajectories. However, it is still unclear whether the nonplanar motion is caused by disturbances in experiments or intrinsically linked to the fluid-body interaction.

In this letter, we report our experimental investigations of free falling thin circular disks in water. The unsteady wake structures were visualized with fluorescence dye and the body trajectories were measured with a stereoscopic vision

method. Our results provide all the six degrees of freedom of falling thin disks over a wide range of the Reynolds number, $Re=Ud/\nu$, and dimensionless moment of inertia, $I^*=\pi\rho_d h/64\rho_f d$. Here U is the averaged falling velocity over long distance, ν is the kinematic viscosity, h and d are thickness and diameter of the disk, and ρ_d and ρ_f stand for the densities of disk and fluid, respectively. Considering that the disks are thin ($h/d \leq 1/10$), we omit the effect of aspect ratio. The disks are made of Plexiglas of density 1.20 g/cm^3. The Reynolds number is determined passively by varying the disk size within 20–60 mm. In the present work, we focus on disks with small I^* values, where path transition from zigzag to spiral and drastic wake structure changes were found.

Initially, a disk was held by an electromagnetic clamp fully immersed in a water tank of $30\times30\times110$ cm^3. As the clamp was opened, the disk started its motion from quiescence. Two charge-coupled device (CCD) cameras (MITRON MTV-1881) were fixed at two opposite locations above the tank, running synchronically at 25 fps, and each camera captured an image sequence of the moving disk. Prior to the measurement, calibrations were carried out in two steps: first the cameras were parametrized for a pinhole model[17] and then the air-water interface position was determined. Dotted markers were made on the disk surface and their pixel coordinates in an image can be estimated to subpixel accuracy. As the pixel coordinates of the markers and their correspondences between a pair of images were known, the six degree-of-freedom pose of the disk could be resolved using the calibration data. The overall reconstruction errors[18] were found to be less than 0.1 mm in the horizontal direction, 0.4 mm in the vertical direction, and 0.6° for orientation. In current setup, the disk appeared in both views of two cameras after descending about 350 mm. The measurement was therefore on the stage significantly beyond the onset of path instability.

Three typical trajectories of the thin disk, including zigzag, transitional, and spiral, were shown in Fig. 1 and the vortex patterns corresponding to the first and third trajecto-
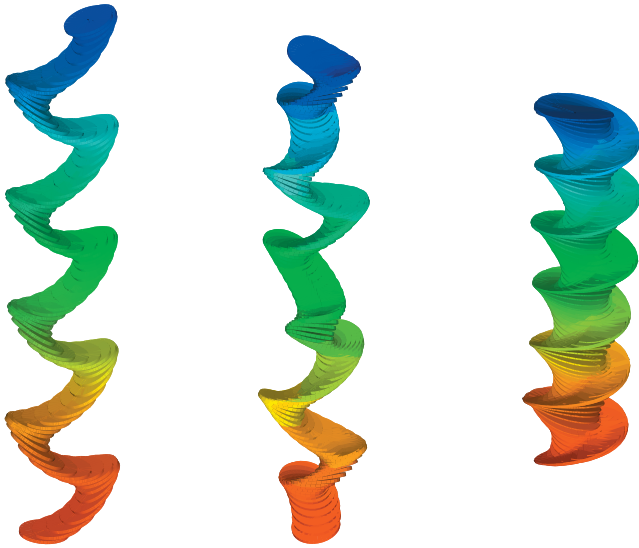
FIG. 1. (Color) Collage of consecutive three-dimensional positions and orientations for falling disks from experiments. Three typical motions are shown, from left to right: planar zigzag ($I^* = 2.95 \times 10^{-3}$, Re=1350, d=30 mm), transitional ($I^* = 1.47 \times 10^{-3}$, Re=935, d=30 mm), and spiral ($I^* = 2.15 \times 10^{-4}$, Re=630, d=28 mm). Time interval Δt is 0.04 s for the zigzag and transitional cases, and Δt is 0.08 s for the spiral case. Color is used to show the distance in the vertical direction.

FIG. 3. (Color) Time evolution of (a) disk center coordinates, (b) Euler angles (ψ, θ, and ϕ stand for gyration, nutation, and self-rotation angles, respectively), and (c) angular velocities for Re=640 and $I^* = 1.99 \times 10^{-4}$.

ries were shown in Fig. 2. In Fig. 2(a), in each cycle, two hairpin vortices shed as the disk moving from one side to the other and the vortical structures were symmetric about the vertical plane. The present observation is consistent with other visualizations of planar zigzag motions.[13,16] Figure 2(b) shows a helicoidal vortex evolution behind a spiraling disk. The flow separation and wake vortices evolution play a sig-
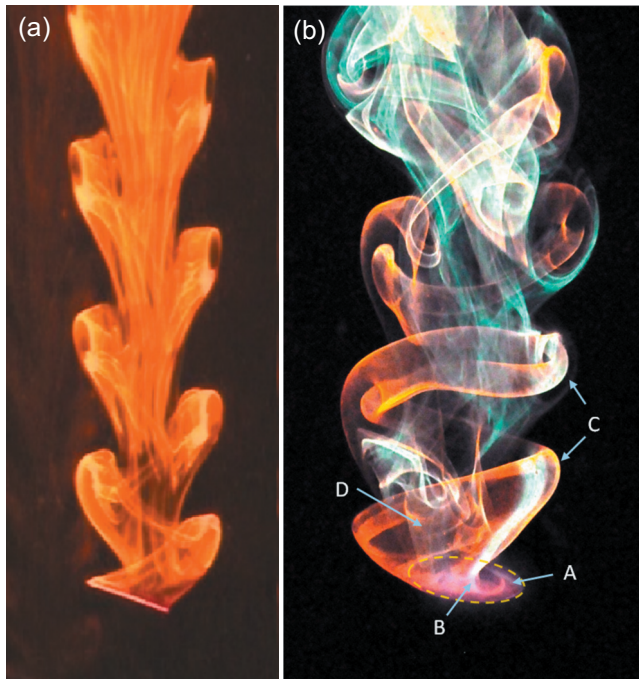

FIG. 2. (Color) The wake structure of the disk is visualized with fluorescence dye. Left: the periodic hairpin vortices shed off from a zigzagging disk for $I^* = 2.95 \times 10^{-3}$ and Re $\approx$ 700. Right: the helicoidal wake is developed behind the disk for $I^* = 3.24 \times 10^{-4}$ and Re $\approx$ 900. The disk edge is highlighted by the dashed line.
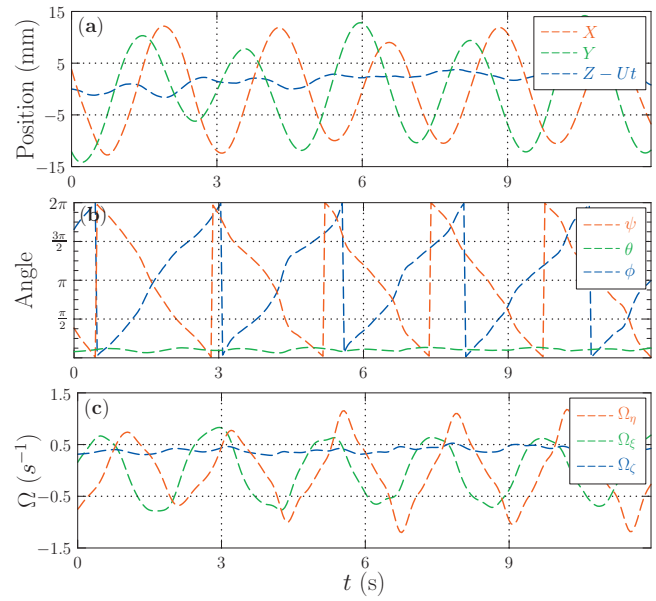
nificant role in disk movement. For a zigzagging disk, the flow separation occurs on the edge of the disk due to the high pressure gradient near the sharp edge. For a disk spiraling around a vertical axis, the side far from the axis has a larger velocity. Therefore by the separation on the edge [shown as arrow A in Fig. 2(b)], more vorticity is produced and feeds into the wake, and subsequently scrolls into a roll. Since the separation location rotates with the disk, the vortex forms a helicoidal shape (arrow C). Meanwhile, the shear layer on the side near to the vertical axis is relatively weak and will be affected by the wake. The downwash flow of the wake causes a separation on the disk surface (arrow B) which is connected to the separation on the edge. The separation generated an upright vortex (arrow D) inside the helicoidal vortex, carrying streamwise vorticity with opposite sign of the helicoidal vortex.

In Fig. 3, we show the time evolutions of the disk center coordinates, three Euler angles and angular velocities for a spiral case when Re=640 and $I^* = 1.99 \times 10^{-4}$. As shown in Fig. 3(a), the variations of the disk center coordinates are sinelike in the horizontal directions x and y. The amplitudes are nearly the same, while the phases are shifted $\pi/2$, implying that the projection of the trajectory on the horizontal plane is circular and coils around the vertical axis. Compared with the zigzag case (not shown here), the oscillation amplitude in the vertical (z) direction is relatively small (the mean velocity of the disk along the z direction has been subtracted). The time evolution of the angular motion is shown in Fig. 3(b). We can see that the nutation angle θ is almost constant with a small variation. It is interesting to notice that the gyration angle ϕ increases and the self-rotation angle ψ decreases almost at constant rates, respectively. For clarity we have used 2π module operator for Fig. 3(b). This type of rotary motion is different from the steady spin of samara[5,19] and aircraft[20] where the self-rotation angle is constant and only gyration occurs.[21] For a rigid body moving in a fluid,
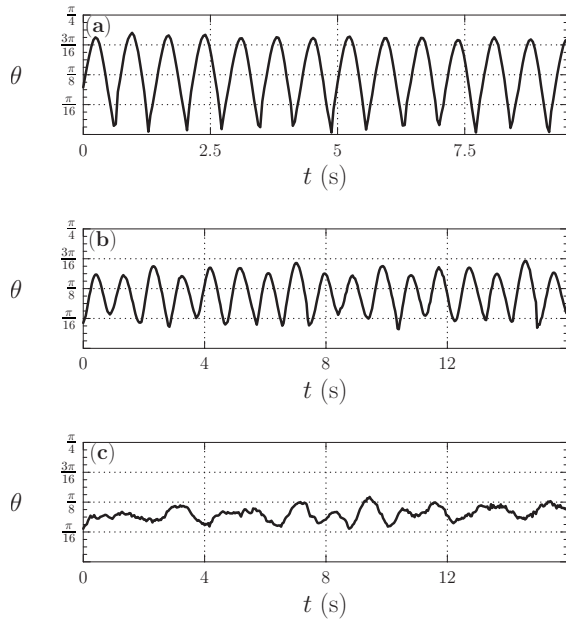
FIG. 4. The measurements of the nutation angle θ. (a), (b), and (c) correspond to the three cases given in Fig. 1.

the torque balance can be described by the generalized Kirchhoff equations as follows:[22]

$$(\mathbb{J} + \mathbb{D})\frac{d\mathbf{\Omega}}{dt} + \mathbf{\Omega} \times (\mathbb{J} + \mathbb{D})\mathbf{\Omega} + \mathbf{U} \times \mathbb{A}\mathbf{U} = \mathbf{\Gamma}^{\text{Vort}}, \qquad (1)$$

where $\mathbb{J}$ is the moment of inertial tensor, while $\mathbf{U}$ and $\mathbf{\Omega}$ are translational and angular velocities. $\mathbb{A}$ and $\mathbb{D}$ stand for the added mass and added inertia tensors, respectively. $\mathbf{\Gamma}^{\text{Vort}}$ represents the torque resulting from the existence of vorticity. As I^* is small, the effects of added mass and moment of inertia play a major role for the disk case, but these are negligible for the samara case.

Figure 3(c) shows the time evolution of disk angular velocities in a frame fixed with the moving disk. Let us denote ζ for the revolution axis, ξ and η for two perpendicular axes on the disk surface. In previous studies,[16,23] the rotation about the revolution axis, Ω_ζ, was observed to be negligible. However, we found Ω_ζ was not small in nonplanar motions. For this case, it is approximately half of the angular velocities about the diameters, Ω_ξ and Ω_η. Due to the symmetry of the body, the components of Eq. (1) in axis ζ can be simplified as

$$J_\zeta \frac{d\Omega_\zeta}{dt} = \Gamma_\zeta^{\text{Vort}}. \qquad (2)$$

This relation indicates that the rotation about the revolution axis is entirely caused by the effect of vorticity. Ω_ζ is also important to the evolution of nonplanar motions. The rotation results in a velocity difference over the spanwise direction of the disk. Then the hydrodynamic lifts on the two lateral sides of the instantaneous velocity become unequal and produce a torque to tilt the body. As the disk is tilted, the horizontal component of the lift plays the role of centrifugal force which causes the nonplanar motion.

In Fig. 4, we present the time evolution of nutation angle θ. Compared with other parameters, θ is more sensitive to
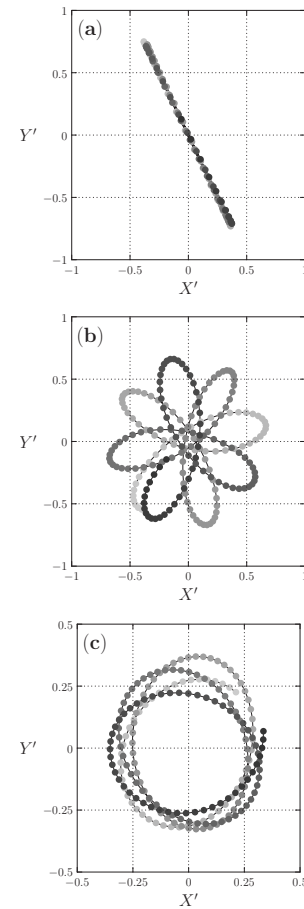

FIG. 5. Top view of disk trajectories corresponding to the cases in Fig. 1. The coordinates are normalized by disk diameter. The bright to dark change represents height change.

the motion transition. For the zigzag, the periodic oscillation of θ is observed, while θ is nearly constant for the spiral motion. Interestingly, a new type of θ evolution is found for intermediate I^* values. In this situation, the maximum values and minimum values changed over different cycles intermittently. For the Reynolds number in our experiments, as long as the nonplanar motion occurs, this phenomenon will occur. The amplitude of oscillation gets smaller while I^* decreases. As the disk motion becomes spiral, the oscillation of θ disappears.

Figure 5 shows the top view of disk center trajectories corresponding to Fig. 4. For the zigzag case, the data points collapse on a line segment, while for the nonplanar cases they form a plane trajectory similar to the rhodonea curve. The curves can be expressed in general by a polar equation of the form

$$r = \mathcal{A}[\cos(k\theta) + \epsilon \sin(k\theta)]. \qquad (3)$$

Thus the planar motion consists of two parts: (1) a harmonic oscillation on an ellipse, with $\mathcal{A}$ being the half length of the long axis and ϵ being the ratio of the short axis to long axis, and (2) a rotation about the vertical direction, with k denoting the ratio of the period of oscillation to the period of rotation. The oscillation part corresponds to the planar zigzag motion with $\epsilon = 0$ and to the spiral motion with $\epsilon = 1$. For intermediate ϵ, the disk motion is named as the transitional
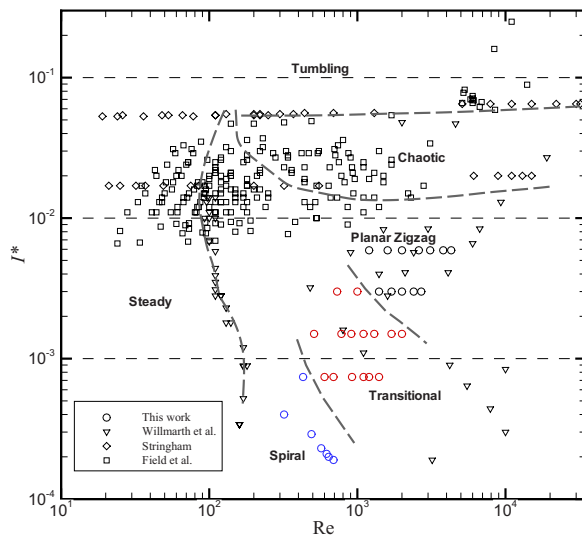
FIG. 6. (Color online) Re−I^* phase diagram for thin circular disks. Circles are from present work, include planar zigzag, transitional and spiral motion, other motions are adapted from Ref. 9.

motion. By Hilbert transform,[16,24] ϵ is determined to be 0.005, 0.07, and 0.77 for the three cases shown in Fig. 5. For the transitional motion, an increase of ϵ with decreasing I^* and Re was also observed.

When the disk starts to move, planar zigzag motion always occurs first. However, the motion is not stable for the disks with smaller I^* values and a secondary oscillation grows in the normal direction. The underlying mechanism is similar to the work by Vandenberghe *et al.*[25] that a vertically oscillating plate induces a horizontal movement. At the same time, the direction of oscillation starts to rotate and the disk starts to spin around the revolution axis. As indicated in Eq. (2), the transition from zigzag to spiral motion tends to happen with smaller I^* since the disk is easier to rotate.

In Fig. 6, we extended the Re−I^* phase diagram of Field *et al.*[9] by adding our results. The regime of periodic motion in the Field *et al.* diagram is replaced by three parts: planar zigzag, transitional, and spiral motion. With limited test cases, the boundaries between each regime were estimated and the influences of I^* and Re are obvious. For increasing Re and I^*, the body trajectory becomes more planar, and for decreasing Re and I^*, the body trajectory becomes more circular. These phenomena were not sensitive to initial tilt. The disk reached the same type of motion as the release angle changed. However, we cannot exclude other nonplanar motions in different parameter regimes.

In summary, the free falling behavior of thin circular disks in quiescent fluid was investigated experimentally. The time-resolved body motions with six degrees of freedom were obtained by a stereoscopic vision method. We therefore identified the different types of disk motion in three dimensions. Particularly, two new types of nonplanar motions, the transitional and spiral motions, were found to occur at small I^* values. With decreasing Re and I^*, the body trajectories changed from planar zigzag to elliptical helix, and eventually to circular helix. The transition was closely related to the rotation about axis of revolution, and the variation of nutation angle from periodic oscillation to constant. By visual-

ization of wake structures, we showed that the spiral motion was induced by the continuous shedding of a pair of counter-rotating vortices with helicoidal shape, whereas the planar zigzag motion was a consequence of periodic shedding of hairpin vortices.

[1] R. List and R. S. Schemenauer, "Free-fall behavior of planar snow crystals, conical graupel and small hail," J. Atmos. Sci. **28**, 110 (1971).

[2] R. E. Stewart and R. List, "Gyrational motion of disks during free-fall," Phys. Fluids **26**, 920 (1983).

[3] G. E. Stringham, D. B. Simons, and H. P. Guy, "The behavior of large particles falling in quiescent liquids," U.S. Geol. Surv. Prof. Pap. **562-c**, 1 (1969).

[4] Z. H. Xia, K. W. Connington, S. Rapaka, P. T. Yue, J. J. Feng, and S. Y. Chen, "Flow patterns in the sedimentation of an elliptical particle," J. Fluid Mech. **625**, 249 (2009).

[5] C. W. McCutchen, "The spinning rotation of ash and tulip tree samaras," Science **197**, 691 (1977).

[6] D. G. Karamanev, C. Chavarie, and R. C. Mayer, "Dynamics of the free rise of a light solid sphere in liquid," AIChE J. **42**, 1789 (1996).

[7] Z. J. Wang, "Dissecting insect flight," Annu. Rev. Fluid Mech. **37**, 183 (2005).

[8] P. G. Saffman, "On the rise of small air bubbles in water," J. Fluid Mech. **1**, 249 (1956).

[9] S. Field, M. Klaus, M. Moore, and F. Nori, "Chaotic dynamics of falling disks," Nature (London) **388**, 252 (1997).

[10] Y. Tanabe and K. Kaneko, "Behavior of a falling paper," Phys. Rev. Lett. **73**, 1372 (1994).

[11] A. Belmonte, H. Eisenberg, and E. Moses, "From flutter to tumble: Inertial drag and Froude similarity in falling paper," Phys. Rev. Lett. **81**, 345 (1998).

[12] L. Mahadevan, W. S. Ryu, and A. D. T. Samuel, "Tumbling cards," Phys. Fluids **11**, 1 (1999).

[13] U. Pesavento and Z. J. Wang, "Falling paper: Navier-Stokes solutions, model of fluid forces, and center of mass elevation," Phys. Rev. Lett. **93**, 144501 (2004).

[14] A. Andersen, U. Pesavento, and Z. J. Wang, "Unsteady aerodynamics of fluttering and tumbling plates," J. Fluid Mech. **541**, 65 (2005).

[15] W. W. Willmarth, N. E. Hawk, and R. L. Harvey, "Steady and unsteady motions and wakes," Phys. Fluids **7**, 197 (1964).

[16] P. C. Fernandes, F. Risso, P. Ern, and J. Magnaudet, "Oscillatory motion and wake instability of freely rising axisymmetry bodies," J. Fluid Mech. **573**, 479 (2007).

[17] Z. Y. Zhang, "A flexible new technique for camera calibration," IEEE Trans. Pattern Anal. Mach. Intell. **22**, 1330 (2000).

[18] H. J. Zhong, "Free falling disks in fluids," Ph.D. thesis, Peking University, 2010.

[19] A. Azuma and K. Yasuda, "Flight performance of rotary seeds," J. Theor. Biol. **138**, 23 (1989).

[20] H. J. Lugt, "Autorotation," Annu. Rev. Fluid Mech. **15**, 123 (1983).

[21] H. J. Zhong and C. B. Lee, "Paths of freely falling disks," Mod. Phys. Lett. B **23**, 373 (2009).

[22] M. Howe, "On the force and moment on a body in an incompressible fluid, with application to rigid bodies and bubbles at high and low Reynolds numbers," Q. J. Mech. Appl. Math. **48**, 401 (1995).

[23] P. Ern, F. Risso, P. C. Fernandes, and J. Magnaudet, "Dynamical model for the buoyancy-driven zigzag motion of oblate bodies," Phys. Rev. Lett. **102**, 134505 (2009).

[24] K. Ellingsen and F. Risso, "On the rise of an ellipsoidal bubble in water: Oscillatory paths and liquid-induced velocity," J. Fluid Mech. **440**, 235 (2001).

[25] N. Vandenberghe, J. Zhang, and S. Childress, "Symmetry breaking leads to forward flapping flight," J. Fluid Mech. **506**, 147 (2004).